Incommensurate ordered phase in non-stoichiometric tantalum carbide

1996 J. Phys.: Condens. Matter 8 8277

(http://iopscience.iop.org/0953-8984/8/43/020)

J. Phys.: Condens. Matter **8** (1996) 8277–8293. Printed in the UK

Incommensurate ordered phase in non-stoichiometric tantalum carbide

A I Gusev, A A Rempel and V N Lipatnikov

Institute of Solid State Chemistry, Ural Division of the Russian Academy of Sciences, Pervomaiskaya 91, 620219 Ekaterinburg, Russia

Received 12 February 1996, in final form 12 April 1996

Abstract. By the neutron diffraction structure analysis method, an ordered phase of non-stoichiometric tantalum carbide TaC_y with the base B1(NaCl) structure has been detected. It is shown that the superstructural reflections observed correspond to an incommensurate superstructure close to M_6C_5 type. With allowance for ordering of TaC_y, the phase diagram of the Ta–C system has been calculated and constructed. The effects of non-stoichiometry and ordering on the period of a base B1-type lattice of tantalum carbide and on the superconducting critical temperature have been studied.

1. Introduction

Disordered non-stoichiometric tantalum monocarbide $TaC_y(TaC_y\square_{1-y})$ has a highly symmetric cubic B1(NaCl)-type structure with statistical distribution of carbon atoms C and structural vacancies $\square$ at non-metallic FCC sublattice sites. Tantalum monocarbide exists over a wide homogeneity region from $TaC_{0.71}$ to $TaC_{1.00}$ [1, 2]. The carbide TaC_y ($1.00 \geqslant y > 0.98$) close to stoichiometry has a superconducting transition temperature $T_c \approx 11$ K [3]. As the carbon content decreases and the vacancy concentration increases, T_c for a disordered carbide TaC_y falls rapidly and reaches about 2 K even for $y = 0.85$.

It is known that a redistribution of carbon atoms and vacancies in non-metallic sublattice sites may under certain conditions give rise to ordered structures. The ordering is accompanied by changes in the physical properties of carbides. For example, the T_c of the ordered carbide $NbC_{0.83}$ turned out to be a factor of nearly four larger than that of the disordered carbide of the same composition [4–7]. Later these results were confirmed [8]. According to [5–7] the higher T_c of ordered niobium carbide is due to features of the M_6C_5-type superstructure formed in NbC_y.

Cubic tantalum carbide TaC_y is one of the non-stoichiometric carbides in which ordering is the most difficult to probe. The fact is that the relative intensity of possible superstructure reflections is very low in x-ray and electron diffraction experiments, in view of the large difference in the scattering amplitudes of carbon and tantalum atoms. In a neutron diffraction experiment, strong absorption of neutrons by the massive tantalum nuclei leads to a considerable lowering of the total intensity of the diffraction spectrum; as a consequence, superstructure reflections are difficult to detect.

An electron diffraction study of $TaC_{0.83}$ [9] has revealed the presence of a diffuse band whose geometry supposedly corresponds to an M_6C_5-type ordering with a very small degree of order. In [10–13] the ordering in tantalum carbide was investigated with the use

0953-8984/96/438277+17$19.50

of neutron diffraction, the magnetic susceptibility method and low-temperature adiabatic calorimetry. The neutron diffraction patterns of annealed TaC_y ($0.79 \leqslant y \leqslant 0.89$) samples exhibited weak superstructure reflections. Judging from this data, an ordered phase close to M_6C_5 type arises in tantalum carbide [11].

The available data on ordering in the non-stoichiometric carbide TaC_y are far from complete. The structure of the ordered phase of tantalum carbide has not been determined in detail and the effect of ordering on the properties of tantalum carbide has been studied insufficiently.

The aim of the present work was to study the crystal structure of the ordered tantalum carbide, to analyse the distribution of carbon atoms and structural vacancies in the superstructure treated and to obtain information about the effect of non-stoichiometry and ordering on the period of a base B1-type lattice and the superconductivity of this compound.

2. Experiment

2.1. Specimens

Specimens of different compositions within the homogeneity region of tantalum carbide were synthesized by solid-phase sintering of metallic tantalum and carbon powders at a temperature of 2500 K in 0.0013 Pa (1×10^{-5} Torr) vacuum for 20 h, followed by cooling to 300 K at a rate of 15 K min^{-1}. X-ray analysis showed that all the TaC_y specimens produced were homogeneous and contained only one phase with a B1 structure. The composition of the tantalum carbide specimens produced was determined by chemical analysis (table 1). The impurity content of the specimens as determined from the results of chemical and spectral analysis did not exceed 0.1 wt%.

To produce tantalum carbide specimens in states with different degrees or ordering, the specimens synthesized were heat treated under various conditions which differed in temperature, annealing time and rate of quenching (figure 1). Annealing at a temperature of 1900 K for 1.5 h followed by quenching at a rate of 2000 K min^{-1} (regime a) was used to obtain specimens in the disordered state. Annealing at 1600 K for 5 h followed by cooling to 750 K at a rate of 0.26 K min^{-1} (regime b) and annealing at 1600 K for 35 h followed by slow cooling to 750 K at a rate of 0.16 K min^{-1} (regime c) were used to reach an equilibrium ordered state of non-stoichiometric tantalum carbide with different degrees of long-range order. The heat treatment regime will be given in parentheses after the carbide composition, e.g. $TaC_{0.83}$ (a).

2.2. X-ray and neutron diffraction experiments

The initial structural determination of the TaC_y specimens investigated was carried out by x-ray analysis in the presence of a standard sample, which allowed the period of the FCC sublattice of tantalum in TaC_y to be measured to within $\pm 0.000\,01$ nm (the standard sample was single-crystal silicon powder with a crystal lattice period $a = 0.543\,086$ nm). X-ray analysis was made on the x-ray automated diffractometer STADI-P with a position-sensitive detector. The tantalum sublattice period for the ordered phase turned out to be larger than that for the disordered carbide of the same composition.

To detect the possible ordering structure, analysis by neutron diffraction was employed. The research water–water atomic reactor, IVV-2M, was used as a slow neutron source. Neutron diffraction measurements were performed with the use of a beam of neutrons of wavelength $\lambda = 0.1694 \pm 0.0002$ nm; the diffractometer resolution $\Delta d/d$ was equal to

Table 1. B1-type lattice period a and superconducting temperature T_c of TaC_y in the disordered and ordered states.

Chemical formula TaC_y	Composition (wt%)			Lattice period a (nm)		Superconducting temperature T_c (K)	
	Ta	C	O	Disordered state	Ordered state	Disordered state	Ordered state
$TaC^{a}_{0.70}$	95.38	4.43	0.16	0.440 00			
$TaC_{0.75}$	94.92	4.73	0.15	0.441 60			
$TaC_{0.76}$	95.06	4.79	0.21	0.441 73			
$TaC_{0.78}$	94.99	4.92	0.19	0.442 20			
$TaC_{0.79}$	94.89	4.98	0.22	0.442 31	0.442 36		
$TaC_{0.80}$	94.82	5.02	0.20	0.442 40	0.442 47		
$TaC_{0.81}$	94.87	5.12	0.18	0.442 45	0.442 60		
$TaC_{0.82}$	94.38	5.14	0.11	0.442 60	0.442 83		
$TaC_{0.83}$	94.75	5.24	0.15	0.442 76	0.443 08	1.5	2.1
$TaC_{0.84}$	94.52	5.27	0.14	0.442 97	0.443 23		
$TaC_{0.85}$	94.87	5.31	0.11	0.443 10	0.443 32		
$TaC_{0.86}$	84.47	5.38	0.15	0.443 26	0.443 47		
$TaC_{0.87}$	94.59	5.47	0.12	0.443 43	0.443 54	2.5	2.8
$TaC_{0.88}$	94.49	5.52	0.12	0.443 60	0.443 70		
$TaC_{0.89}$	94.29	5.57	0.21	0.443 70	0.443 76		
$TaC_{0.90}$	94.24	5.63	0.18	0.443 96		3.7	
$TaC_{0.92}$	94.07	5.75	0.20	0.444 44		4.4	
$TaC_{0.93}$	94.05	5.81	0.21	0.444 51			
$TaC_{0.94}$	94.05	5.87	0.12	0.444 65		6.0	
$TaC_{0.95}$	93.98	5.90	0.11	0.444 97			
$TaC_{0.96}$	93.77	5.97	0.22	0.444 98		8.7	
$TaC_{0.98}$	93.68	6.09	0.16	0.445 30			
$TaC_{0.99}$	93.67	6.16	0.15	0.445 49			
$TaC_{1.00}$	93.78	6.23	0.11	0.445 55		10.1	

[a] $TaC_{0.70}$ contains cubic TaC_y and hexagonal Ta_2C_y phases; period of a cubic B1-type phase is given in table 1.

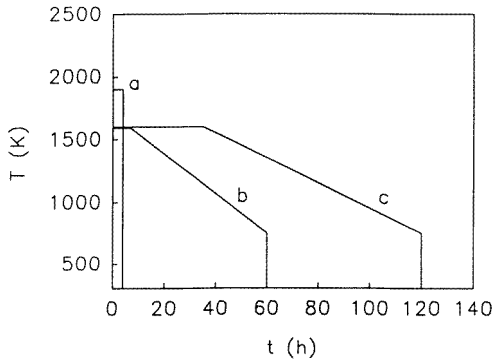

Figure 1. Heat treatment conditions used to produce TaC_y with different degrees of ordering.

0.01. The beam was monochromated by reflection of neutrons from the (111) plane of a germanium single crystal. The recording system consisted of ten helium detectors SNM-16 of slow neutrons and a multichannel analyser AI-4096. Neutron diffraction patterns were taken at room temperature in the angular interval $12^\circ \leqslant 2\Theta \leqslant 90^\circ$ in the step scanning

regime with the quantity $\Delta(2\Theta) = 0.1^\circ$ in the step scanning regime with the quantity $\Delta(2\Theta) = 0.1^\circ$. Neutron diffraction patterns were identified for a base B1-type lattice using the parameter 0.4428 nm determined by the x-ray method.

The heavy tantalum nuclei are strong absorbers of neutrons, and so, to detect the weak superstructure reflections with an intensity of about 1% of the $(200)_{B1}$ structural reflection, a large accumulation was made at each scanning step (the background intensity was about 5000 counts). Taking this into account, the neutron diffraction patterns were interpreted with allowance for the presence of parasitic reflections (from wavelengths $\lambda/2$ and $\lambda/3$) corresponding to structural reflections $(200)_{B1}$, $(220)_{B1}$ and $(222)_{B1}$. The intensity of parasitic reflections was about 0.5% relative to that of the main reflection. For tantalum carbide with a base lattice period $a_{B1} = 0.4428$ nm, the parasitic reflections were observed at $2\Theta = 14.7^\circ$, 20.8°, 22.1°, 25.5°, 29.5° and 31.4°, their intensity being independent on the regime of heat treatment.

2.3. Superconducting measurements

The transition temperature T_c to the superconducting state was measured by the inductive method. The measurements were made with specimens of the stoichiometric carbide $TaC_{1.00}$, the quenched non-stoichiometric carbides $TaC_{0.96}$, $TaC_{0.94}$, $TaC_{0.92}$, $TaC_{0.90}$, $TaC_{0.87}$ and $TaC_{0.83}$, and annealed specimens of the carbides $TaC_{0.87}$ and $TaC_{0.83}$. The error of measurement for T_c was 0.1 K for $T_c > 4.2$ K and 0.4 K for $T_c < 4.2$ K.

3. Structure of the ordered phase

3.1. Confirmation of the ordered structure

Neutron diffraction patterns were recorded of both quenched and annealed tantalum carbide specimens of all the compositions synthesized. Figure 2 shows typical diffraction patterns in the angle range where additional reflections were observed side by side with the $(111)_{B1}$ structural reflection corresponding to $2\Theta \approx 39^\circ$. The low intensity of this structural reflection lies at the level of the superstructure reflections, since for TaC_y the intensity of the $(111)_{B1}$ reflection is proportional to the $(f_{Ta} - yf_C)^2$, and the amplitude f_{Ta} of the atomic scattering of tantalum and the amplitude f_C of the scattering of carbon are of similar magnitudes ($f_{Ta} = 0.7 \times 10^{-12}$ cm; $f_C = 0.665 \times 10^{-12}$ cm).

The first additional reflection ($2\Theta \approx 14.7^\circ$), which occurs in all the neutron diffraction patterns, is parasitic. All diffraction patterns also show two other parasitic reflections corresponding to $2\Theta \approx 20.8^\circ$ and 22.1°. These two are superimposed on the diffuse-scattering peak at $2\Theta \approx 20$–23°. The peak of diffuse scattering occurs in the neutron diffraction patterns for all TaC_y specimens except $TaC_{1.00}$ and indicates the presence in them of some short-range order with $\alpha_{1,2} < 0$ (α_1 and α_2 being the short-range order parameters for the first and second coordination spheres, respectively, of the non-metallic sublattice). In the same angle range, $2\Theta \approx 20$–23°, the neutron diffraction patterns for TaC_y specimens containing an ordered phase also have superstructure reflections. Thus the broad maximum at $2\Theta \approx 20$–23° in the neutron diffraction patterns (figure 2) includes several components depending on the composition and heat treatment of carbide.

Superstructure reflections with intensity depending on the heat treatment of specimens were observed in neutron diffraction patterns of annealed carbide TaC_y in the composition range $TaC_{0.79}$–$TaC_{0.89}$. Note that the weak superstructure reflections appear also for the quenched carbide $TaC_{0.83}$ (a) (figure 2). This indicates that the quench rate used

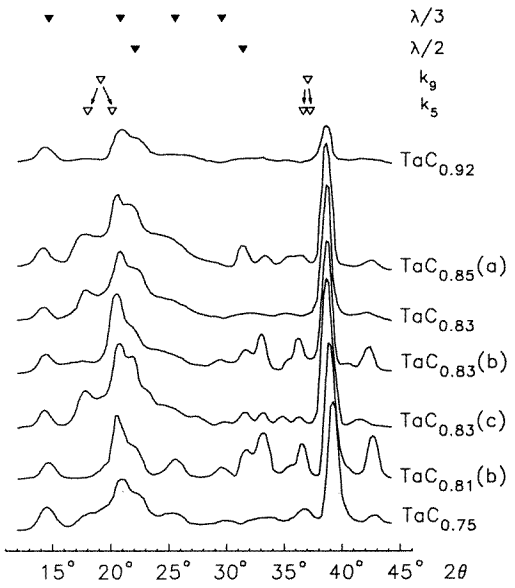

Figure 2. Neutron diffraction patterns of TaC_y in different structural states upon heat treatment under regimes a, b and c: ▼, positions of the reflections due to parasitic radiation with wavelengths $\lambda/2$ and $\lambda/3$; ▽, positions of the superstructural reflections corresponding to the star $\{\boldsymbol{k}_5\}$; the arrows show the splitting of the reflections referring to the star $\{\boldsymbol{k}_9\}$, which are observed in the spectra of commensurate M_6C_5-type superstructures, into the experimental superstructural reflections corresponding to the star $\{\boldsymbol{k}_5\}$.

(200 K min^{-1}) was not sufficient to obtain tantalum carbide in the disordered state. Investigations showed that the width of the superstructure reflections exceeded that of the structural reflection $(111)_{B1}$, their intensity decreased rapidly with increasing diffraction angle 2Θ and the superstructure reflections become almost invisible for $2\Theta > 50^\circ$. These results are evidence that the ordered phase domains are much smaller than the grains of disordered carbide with a base B1-type structure. The features mentioned suggest that, even after prolonged annealing (regime c), ordering in tantalum carbide does not form a structure with ideal long-range order, although ordering proceeds fairly quickly.

In the neutron diffraction patterns of tantalum carbide, there is an angle range $2\Theta = 19$–25° corresponding to wavevectors that restrict the first Brillouin zone of the FCC non-metallic sublattice. The presence of superstructure reflections in and near this angle range indicates that static concentration waves with wavevectors terminating near the boundary of the first Brillouin zone arise in the crystal. According to [1, 2, 6, 14, 15], ordering in cubic non-stoichiometric monocarbides of group V transition metals gives rise predominantly to M_6C_5-type phases or phases close to them. Earlier [16] we have determined the $MC_{0.83}$–M_6C_5 disorder–order phase transition channels for the known commensurate M_6C_5-type superstructures (figure 3). Taking this into account, the positions of the superstructure reflections for the known ordered M_6C_5-type structures with space groups $C2/m$, $P3_1$ and $C2$ were calculated; calculation was performed for a base B1-type lattice using the period $a_{B1} = 0.4428$ nm corresponding to disordered $TaC_{0.83}$. From a comparison of the calculated and observed superstructure reflection positions it follows that the tantalum carbide superstructure found differs from the known M_6C_5-type superstructures. What could be the reason for this?

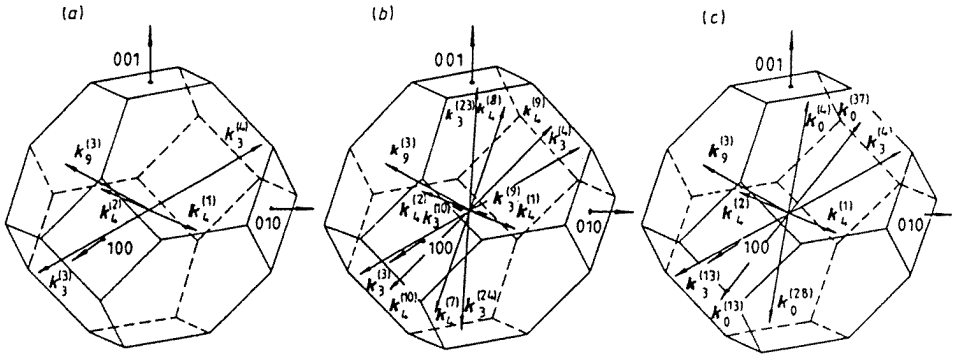

Figure 3. Superstructure vectors of the reciprocal lattice of ordered M_6C_5-type structures, involved in the $MC_{0.83}$–M_6C_5 disorder–order phase transition channel, and the position of these vectors in the first Brillouin zone of the FCC lattice: (a) monoclinic ordered structure (space group, $C2/m$); (b) trigonal ordered structure (space group, $P3_1$); (c) monoclinic ordered structure (space group, $C2$).

If one takes into account only the non-metallic sublattice, a common feature of all ideal M_6C_5-type superstructures (space groups $C2/m$, $P3_1$ and $C2$) is that complete (defect-free) and partially filled (defective) ordered carbon planes alternate in the $[1\bar{1}1]_{B1}$ direction (or in the equivalent directions $[111]_{B1}$, $[\bar{1}11]_{B1}$ and $[1\bar{1}1]_{B1}$, depending on the unit-cell orientation). In the complete planes, all the sites are occupied by carbon atoms. The partially filled ordered planes contain both carbon atoms and vacancies; in these planes, two thirds of all the sites are occupied by carbon atoms, one third of all the sites are vacant and each vacancy is surrounded by six carbon atoms that form a regular hexagon. The difference between the aforementioned ideal M_6C_5-type superstructures is associated with different plane-parallel relative displacements of defective $(1\bar{1}1)_{B1}$ planes for each of these three superstructures [6, 16, 17].

The alternation of complete and defective non-metallic $(1\bar{1}1)_{B1}$ planes in ordered M_6C_5-type structures arises because the arm $\boldsymbol{k}_9^{(3)} = \boldsymbol{b}_2/2$ of the star $\{\boldsymbol{k}_9\}$ is present in the disorder–order transition channels [6, 16]. (Here and henceforth the subscript of the wavevector corresponds to the star number, and the superscript refers to the arm number; the stars and their arms are numbered according to [6, 18]; $\boldsymbol{b}_2 = \langle 1\bar{1}1\rangle$ is one of the basis vectors of the reciprocal lattice of an FCC crystal (in units $2\pi/a_{B1}$)). The star $\{\boldsymbol{k}_9\}$ ensures the commensurability of such ordered structures since the interplanar distance corresponding to it coincides with one of the interplanar distances of the disordered base B1-type structure.

A comparison of neutron diffraction patterns of tantalum carbide with diffraction spectra of M_6C_5-type superstructures considered has revealed that the spectrum of tantalum carbide does not contain reflections at $2\Theta = 19.0^\circ$, 37.0°, 59.0°, etc, that correspond to the star $\{\boldsymbol{k}_9\}$ of the FCC non-metallic sublattice. These reflections in the diffraction patterns of tantalum carbide are split into two superstructure reflections (satellites), e.g. $2\Theta = 18.0^\circ$ and 20.5° (figure 2). An analysis of the satellite position in the diffraction patterns indicates that the satellites may belong to the star $\{\boldsymbol{k}_5\}$. The arms of the star $\{\boldsymbol{k}_5\}$ are collinear to those of the star $\{\boldsymbol{k}_9\}$ and do not reach the boundary of the first Brillouin zone; they have the running index $0 < \mu_5 < 1/2$ (figure 4). In the general case, the position of the arms $\boldsymbol{k}_5^{(j)}$ may vary continuously from the zero point of reciprocal space to the points L on the boundary of the first Brillouin zone; points L correspond to the arms of the star $\{\boldsymbol{k}_9\}$. The presence of the

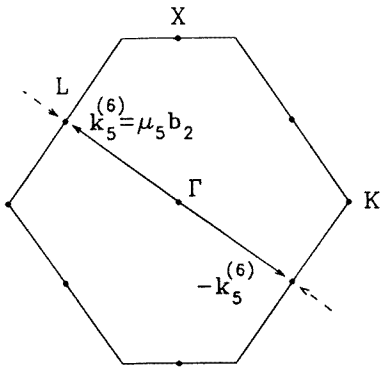

Figure 4. Position of the superstructure vectors $\boldsymbol{k}_5^{(6)}$ and $-\boldsymbol{k}_5^{(6)}$ in the (110) section of the first Brillouin zone; the superstructure vectors $\boldsymbol{k}_5^{(j)}$ indicated by dotted lines are generated by the nearest sites of the reciprocal lattice. The fact of existence of two superstructure vectors $\boldsymbol{k}_5^{(j)}$ with $\mu_5 \approx 0.473$ near point L leads to the appearance of two superstructure reflections close to each other in the diffraction patterns at $2\Theta \approx 18^\circ$ and 20.5°. (Γ, K, L and X are the special points of the first Brillouin zone.)

arms of the star $\{\boldsymbol{k}_5\}$ in the phase transition channel actually denotes incommensurability of the superstructure in tantalum carbide.

The numerical value of μ_5 may be derived from the experimental neutron diffraction patterns (figure 2). The arm $\boldsymbol{k}_9^{(3)}$ is collinear to the arm $\boldsymbol{k}_5^{(6)} = \{\mu_5, -\mu_5, \mu_5\}$. The diffraction vector $\boldsymbol{q}$ coincides with the wavevector $\boldsymbol{k}_5^{(6)}$ and has the modulus $|\boldsymbol{q}| = |\boldsymbol{k}_5^{(6)}| = \sqrt{3}\mu_5$. Hence, with $q = (2a_{B1}\sin\Theta)/\lambda$, we obtain

$$\mu_5 = (2a_{B1}\sin\Theta_5)/\sqrt{3}\lambda \tag{1}$$

where $\Theta_5 \approx 9.00$–9.02° is the angle which corresponds to the superstructure reflection due to the wavevector with length $|\boldsymbol{k}_5^{(6)}|$. The calculation gave $\mu_5 \approx 0.473$, irrespective of TaC_y composition (within the accuracy of diffraction experiment). Also, there is in the first Brillouin zone an opposite superstructural vector $\boldsymbol{k}_5^{(5)} = -\boldsymbol{k}_5^{(6)}$ corresponding to the superstructural vector $\boldsymbol{k}_5^{(6)}$. The vector $\boldsymbol{k}_5^{(5)}$ is not equivalent to the vector $\boldsymbol{k}_5^{(6)}$ and therefore it is involved in the phase transition channel as well as the vector $\boldsymbol{k}_5^{(6)}$. Thus, the disorder–order phase transition channel associated with the formation of incommensurated ordered phase in tantalum carbide includes the arms $\boldsymbol{k}_5^{(6)} \approx 0.473\boldsymbol{b}_2$ and $\boldsymbol{k}_5^{(5)} = -\boldsymbol{k}_5^{(6)}$ (figure 4).

3.2. Distribution of carbon atoms and vacancies

Let us write the function which describes the probability of detecting a carbon atom at the site of the non-metallic $(1\bar{1}1)_{B1}$ plane, i.e. carbon-atom occupancy of the non-metallic $(1\bar{1}1)_{B1}$ plane in MC_y with any degree of long-range order. For commensurate M_6C_5-type superstructures with allowance for the corresponding carbon-atom distribution functions [6, 16, 19] the carbon-atom occupancy $P^{(1\bar{1}1)}$ is

$$P_C^{(1\bar{1}1)} = y - (\eta_9/6)\cos(2\pi\mu_9 z) \tag{2}$$

where z is the ordinal number of the non-metallic plane $(1\bar{1}1)_{B1}$, η_9 is the long-range order parameter corresponding to the star $\{\boldsymbol{k}_9\}$, and $\mu_9 = 1/2$.

For an incommensurate ordered structure close to M_6C_5 type the carbon-atom occupancy of the non-metallic $(111)_{B1}$ plane in MC_y has the analogous form

$$P_{inc}^{(1\bar{1}1)} = y - (\eta_5/6)\cos(2\pi\mu_5 z). \tag{3}$$

It follows from equations (2) and (3) that the maximum value of carbon-atom occupancy is $P_{max}^{(1\bar{1}1)} = y + \eta/6$ and the minimum value is $P_{min}^{(1\bar{1}1)} = y - \eta/6$ with η equal to η_9 or η_5 for the commensurate and incommensurate superstructures, respectively.

The functions $P^{(1\bar{1}1)}$ for the commensurate and incommensurate ordered M_6C_5-type structures are shown in figure 5. It should be noted that these functions have a physical meaning only for the $(1\bar{1}1)_{B1}$ plane.

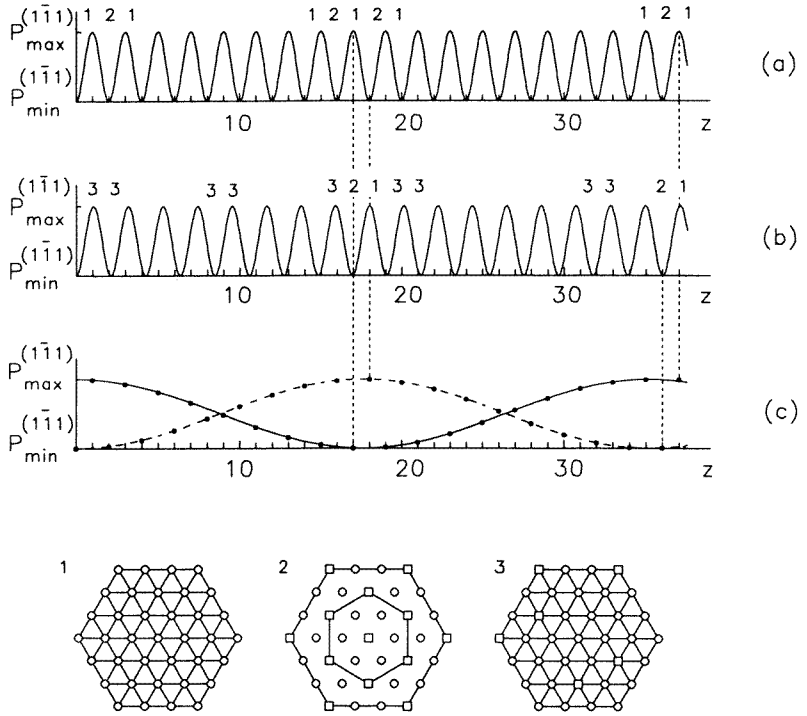

Figure 5. Carbon-atom occupancy $P^{(1\bar{1}1)}$ of the non-metallic atomic $(1\bar{1}1)_{B1}$ planes in the direction $[1\bar{1}1]_{B1}$ (z is the ordinal number of the non-metallic planes $(1\bar{1}1)_{B1}$): (a) commensurate M_6C_5-type superstructure; (b) tantalum carbide incommensurate superstructure close to M_6C_5 type; (c) carbon-atom occupancy $P^{(1\bar{1}1)}$ of odd (——) and even (– – –) non-metallic planes $(1\bar{1}1)_{B1}$ in incommensurate ordered tantalum carbide TaC_y; 1, complete non-metallic plane $(1\bar{1}1)_{B1}$ with maximum carbon-atom occupancy $P_{max}^{(1\bar{1}1)} = y + \eta/6$; 2, defective ordered non-metallic plane $(1\bar{1}1)_{B1}$ with minimum carbon-atom occupancy $P_{min}^{(1\bar{1}1)} = y - \eta/6$; 3, defective non-metallic plane $(1\bar{1}1)_{B1}$ with carbon-atom occupancy intermediate between $P_{max}^{(1\bar{1}1)}$ and $P_{min}^{(1\bar{1}1)}$; ○, carbon atoms; □, vacancies.

As can be seen from figure 5, the non-metallic atomic $(1\bar{1}1)_{B1}$ planes with only the maximum carbon-atom occupancy $P_{max}^{(1\bar{1}1)}$ and minimum carbon-atom occupancy $P_{min}^{(1\bar{1}1)}$ alternate in the $[1\bar{1}1]_{B1}$ direction in the commensurate M_6C_5-type superstructure; these planes will be called type 1 and type 2 planes, respectively. For the incommensurate

superstructure (figure 5(b)), the maxima and minima of the function $P^{(1\bar{1}1)}$ do not coincide with the non-metallic $(1\bar{1}1)_{B1}$ planes and therefore carbon-atom occupancy of these planes is intermediate between the $P^{(1\bar{1}1)}_{max}$ and $P^{(1\bar{1}1)}_{min}$ (figure 5(c)). In other words, the concentration wave corresponding to the star $\{\boldsymbol{k}_5\}$ has maxima and minima which do not coincide with the non-metallic $(1\bar{1}1)_{B1}$ planes. Figure 5(c) shows that in the incommensurate tantalum carbide each seventeenth to eighteenth non-metallic $(1\bar{1}1)_{B1}$ plane has the maximum occupation by carbon atoms (e.g. first eighteenth, thirty-seventh, fifty-fourth, seventy-third, etc). In the commensurate M_6C_5-type superstructure the non-metallic $(1\bar{1}1)_{B1}$ planes with the maximum carbon-atom occupancy (i.e. type 1 plane) encountered every other $(1\bar{1}1)_{B1}$ plane, i.e. first, third, fifth, etc (figure 5(a)). Thus the translation period in the $[1\bar{1}1]_{B1}$ direction increases by a factor of about 18, from 0.5112 nm for a commensurate M_6C_5-type phase to 8.9–9.1 nm in an incommensurate ordered tantalum carbide. The period of translation depends largely on the tantalum carbide composition and heat treatment conditions.

The non-coincidence of the concentration wave maxima and minima with the non-metallic sublattice $(1\bar{1}1)_{B1}$ planes signifies also that the filling probabilities for the carbon and vacancy positions in an ordered tantalum carbide differ appreciably from 1 and 0, respectively. As a consequence, the degrees of long-range and short-range order in an ordered tantalum carbide are far from maximum possible values.

When the long-range order parameters are equal, $\eta_9 = \eta_5 = \eta$, the difference between the carbon-atom occupancies of non-metallic $(1\bar{1}1)_{B1}$ planes in the incommensurate and commensurate superstructures is

$$P^{(1\bar{1}1)}_{inc} - P^{(1\bar{1}1)}_{c} = -(\eta/3)\sin[\pi z(\mu_9 + \mu_5)]\sin[\pi z(\mu_9 - \mu_5)]. \tag{4}$$

Let us estimate in which $(1\bar{1}1)_{B1}$ planes of the non-metallic sublattice the probabilities $P^{(1\bar{1}1)}_{inc}$ and $P^{(1\bar{1}1)}_{c}$ for the incommensurate and commensurate superstructures will be the same. In such a case, $P^{(1\bar{1}1)}_{inc} - P^{(1\bar{1}1)}_{c} = 0$, and equation (4), with the numerical values for μ_9 and μ_5 shows that $z \approx 37m$, where $m = 0, 1, 2, \ldots$ is an integer. Therefore the carbon-atom occupancies of the non-metallic $(1\bar{1}1)_{B1}$ planes in the incommensurate and commensurate M_6C_5-type superstructures are the same for every thirty-seventh plane (figure 5(c)).

In principle, one other possible version exists to explain the distribution of carbon atoms and vacancies in ordered TaC_y. The ordered structure of a non-stoichiometric carbide TaC_y can be represented as the sequences $[(CD)_nC]_\infty$ or $[(CD)_nD]_\infty$ of alternating complete C and ordered defective D non-metallic $(1\bar{1}1)_{B1}$ planes, i.e. as a long-period structure. For a long-period structure $[(CD)_nC]_\infty$ or $[(CD)_nD]_\infty$, the parameter μ_5 should depend on the composition of TaC_y; however, this dependence is not observed within the accuracy of the diffraction experiment that has been performed.

The incommensurability of the structure means the absence of the exact stoichiometric composition of the ordered phase (this does not signify that any ordered phase of non-stoichiometric composition is incommensurate). This explains, in particular, the weak dependence of the superstructure reflection intensities on the composition of TaC_y (figure 2).

3.3. Period of a base B1-type lattice

Measurements showed that a base B1-type lattice period of ordered tantalum carbide is greater than for the quenched disordered carbide TaC_y of the same composition. A similar effect was observed previously for titanium [20], niobium [6, 21] and vanadium [22, 23] carbides.

Figure 6 shows the variation with carbon content of a base lattice period of a disordered and ordered tantalum carbide. An increasing vacancy concentration is accompanied by a non-linear decreasing lattice period a_{B1} of TaC_y. The data on the lattice period of a disordered ($\eta = 0$) tantalum carbide TaC_y were approximated by a second-order polynomial

$$a(y, 0) = a_0 + a_1 y + a_2 y^2 \tag{5}$$

with $a_0 = 0.421\,31$, $a_1 = 0.034\,17$ and $a_2 = -0.009\,92$ nm.

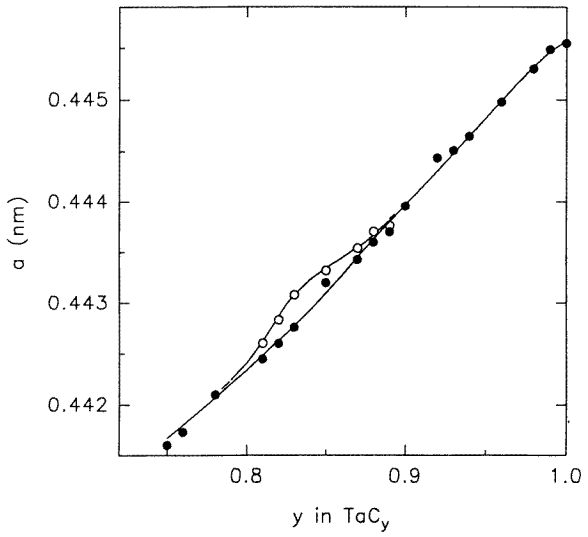

Figure 6. The dependence of the period of a base B1-type crystal lattice on the composition of a disordered (●) and ordered (○) tantalum carbide TaC_y.

Experimentally, the appearance of structural vacancies in disordered carbide is evident from the reduction in lattice period a_{B1} whereas ordering is accompanied by an increase in the base lattice period a_{B1} of carbide. Ordering is observed at a comparatively high vacancy concentration ($0.11 < 1 - y \leqslant 0.21$). At such a concentration the vacancy perturbation regions overlap and partially compensate one another. In an ordered carbide, nearest-neighbour structural vacancies are absent; so this overlap is significantly less than in a disordered carbide. It is easy to understand that a base lattice period increase is possible only when metallic atoms move away from the vacancy. In contrast, if they move towards it, the base lattice period of an ordered carbide should be less than that of a disordered carbide.

Thus an increase in the base lattice period of an ordered carbide compared with a disordered carbide and a reduction in the lattice period with increasing vacancy concentration are possible when two conditions are realized simultaneously: firstly if the metal atoms forming the first coordination sphere of vacancy move away from the vacancy, and secondly if the crystal lattice perturbations due to the vacancy extend over no fewer than two coordination spheres. This is consistent with the experimental data on the static displacements of metal atoms; in non-stoichiometric titanium, zirconium and niobium carbides the metal atoms of the first coordination sphere move away from the vacancy [24, 25]; according to [26], in NbC_y the niobium atoms in the first coordination sphere move away from the vacancy and those in the second sphere move towards the vacancy.

Let us consider a phenomenological model to analyse the increase in lattice period on ordering of non-stoichiometric tantalum carbide. In non-stoichiometric carbides with a base B1(NaCl)-type structure, each metal atom has an environment of six non-metallic sublattice sites which can either be occupied by carbon atoms or be vacant. This allows us to represent the non-stoichiometric carbide MC_y with B1-type structure as a set of clusters in the form of the Dirichlet–Voronoi polyhedron, with a distorted Wigner–Seitz cell. Each cluster contains a metal atom and six non-metallic sublattice sites. Such clusters fill the entire volume of the crystal and account for all the lattice sites.

As a first approximation let us assume that the cluster volume V_m depends only on the number of vacancies in it and is independent of their mutual arrangement. In this case the crystal volume V may be represented as

$$V = N \sum_{m=0}^{6} \lambda_m P_m(y, \eta) V_m \tag{6}$$

where $P_m(y, \eta)$ is the probability that a cluster with a number of vacancies equal to m occurs in the crystal, $\lambda_m = C_6^m$ is the multiplicity of m configuration of the cluster and N is the total number of metallic sublattice sites. On the other hand, the crystal volume may be written in terms of the base lattice period $a_{B1}(y)$ as $V = (N/4)a^3(y)$. Allowing for this and equations (5) and (6), we obtain for a disordered carbide

$$\sum_{m=0}^{6} \lambda_m P_m(y, 0) V_m = \frac{(a_0 + a_1 y + a_2 y^2)^3}{4} \tag{7}$$

where $P_m(y, 0) = (1 - y)^m y^{(6-m)}$ is the probability of formation of a cluster with m vacancies in a disordered carbide. The solution to equation (7) is an expression for the cluster volume V_m:

$$V_m = \tfrac{1}{4} \sum_{k=m}^{6} A_{6-k} \frac{k!(6-m)!}{6!(k-m)!} \tag{8}$$

where A_{6-k} are the coefficients of y^k on the right-hand side of equation (7). For equilibrium conditions, the probability $P_m(y, \eta)$ that a cluster exists in the crystal with any degree of long-range order [1, 6, 14] has the form

$$P_m(y, \eta) = (1/6)[(6-m)n_1 n_2^{(5-m)}(1 - n_2)^m + m(1 - n_1)n_2^{(6-m)}(1 - n_2)^{(m-1)}] \tag{9}$$

where $n_1 = y - 5\eta/6$ and $n_2 = y + \eta/6$ are the probabilities of finding a carbon atom on a vacancy sublattice site or on a carbon sublattice site, respectively, as the M_6C_5-type superstructure is forming.

Using equations (6), (8) and (9), one can find the crystal volume and hence the period of a base B1-type lattice for non-stoichiometric carbide with any degree of order. Calculation of the base lattice period of ordered tantalum carbide was carried out in two ways.

In the first approach it was assumed that the maximum possible degree η_{max} of long-range order in tantalum carbide is achieved. According to [1, 6, 16], the dependence of η_{max} on the composition of MC_y during the formation of an ordered M_6C_5-type phase or incommensurate ordered phase close to M_6C_5 type has the form

$$\eta_{max}(y) = \begin{cases} 6(1-y) \\ 6y/5 \end{cases} \qquad \text{if} \begin{cases} y \geqslant 5/6 \\ y < 5/6. \end{cases} \tag{10}$$

In the second approach it was assumed that in ordered tantalum carbide the long-range order parameter has the same value as at the disorder–order transition temperature T_{trans},

i.e. $\eta = \eta_{trans}$. The η_{trans}-values for the disorder–order MC_y–M_6C_5 transition have been given in [1].

Comparison of the experimental and calculated values of $\Delta a = a(y, \eta) - a(y, 0)$ (table 2) shows that the values obtained in the $\eta = \eta_{trans}$ approximation are nearest to the experimental values. Thus, ordered incommensurate tantalum carbide has the degree of long-range order that corresponds to the thermodynamically equilibrium distribution of carbon atoms and structural vacancies in the crystal lattice. Note that the change in the lattice period of tantalum carbide during ordering is comparable with lattice period change within that part of the homogeneity region of TaC_y where the ordered phase forms; in the region $TaC_{0.81}$–$TaC_{0.89}$, the change in lattice period is 0.0014 nm whereas the maximum ordering-induced change is equal to 0.0005 nm. Thus, the effects of non-stoichiometry and ordering on a base lattice period of TaC_y are comparable in magnitude.

Table 2. Change Δa in a base B1-type lattice period, during ordering of non-stoichiometric tantalum carbide TaC_y.

	Δa (nm)		
		Calculation	
Chemical formula	Experimental	$\eta = \eta_{trans}$	$\eta = \eta_{max}$
$TaC_{0.79}$	0.000 05	0.000 10	0.000 23
$TaC_{0.81}$	0.000 15	0.000 10	0.000 25
$TaC_{0.82}$	0.000 23	0.000 11	0.000 25
$TaC_{0.83}$	0.000 32	0.000 11	0.000 26
$TaC_{0.84}$	0.000 26	0.000 10	0.000 24
$TaC_{0.85}$	0.000 22	0.000 10	0.000 21
$TaC_{0.87}$	0.000 11	0.000 08	0.000 16
$TaC_{0.88}$	0.000 10	0.000 08	0.000 14
$TaC_{0.89}$	0.000 06	0.000 07	0.000 12

The change in a base lattice period during ordering of TaC_y indicates that the disorder–order trnsition is the first-order phase transformation.

4. Phase diagram for the Ta–C system

Order–disorder structural phase transitions in $MX_y\square_{1-y}$ non-stoichiometric interstitial compounds such as transition-metal carbides MC_y may be described by the order parameters functional (OPF) method [1, 6, 14, 27, 28]. The physical basis of this method is the mean-field approximation; as regards its formalism, it is a cluster method but differs in allowing a detailed treatment of a symmetry of a crystal with any degree of long-range order.

The use of the OPF method would allow both qualitative and quantitative description of first-order and second-order structural phase transitions of the order–disorder type in non-stoichiometric carbides MC_y, and a determination of the thermodynamic equilibrium types of superstructures in them [1, 2, 6]. An application of the OPF method for calculating equilibrium phase diagrams of systems in which disorder–order transformations take place have been described in detail in [1, 15]. The numerical values of the energy parameters needed to calculate the phase diagram of the Ta–C system have been given in [1, 15, 29]. In this system, as well as the cubic carbide TaC_y with a wide homogeneity region, there exists a hexagonal lower carbide $\alpha - Ta_2C$ with a narrow homogeneity region. The

existence of a homogeneity region of $\alpha - Ta_2C$ was neglected when calculating the phase diagram. Also, in the Ta–C system a high-temperature carbide $\zeta - Ta_4C_3$ exists which is an autonomous phase of this system. According to different data, $\zeta - Ta_4C_3$ exists over the temperature range 2100–2600 or 2000–2800 K. $\zeta - Ta_4C_3$ has a rhombohedral structure and is not the ordered phase of non-stoichiometric TaC_y with a base B1-type structure.

In the general case, ordered phases of the type M_2X, M_3X_2, M_4X_3, M_6X_5 and M_8X_7 are liable to form (from the viewpoint of crystallography) in non-stoichiometric compounds. To ascertain which ordered phases can really form in TaC_y, the free energies of the disordered phase TaC_y and of the expected ordered phases Ta_2C, Ta_3C_2, Ta_4C_3, Ta_6C_5 and Ta_8C_7 were calculated for temperatures from 700 to 1600 K. At 700 K the ordered Ta_4C_3 phase cannot occur because its $T_{trans} < 600$ K for $0.5 \leqslant y \leqslant 1.0$. At 700 K, ordered Ta_2C, Ta_3C_2 and Ta_6C_5 phases and disordered carbide TaC_y (at $y > 0.96$) possess the lowest free energy in different concentration ranges. The free energy of the possible ordered Ta_8C_7 phase is larger than that of other ordered phases over the entire region of homogeneity of TaC_y ($0.5 \leqslant y \leqslant 1.0$); therefore the ordered Ta_8C_7 phase cannot occur. At a temperature higher than 1430 K, it is only a disordered phase that can exist in the entire homogeneity region of TaC_y.

On the whole, as follows from the calculation, in the temperature interval from 300 to 1400 K the Ta_6C_5 and TaC_y phases and two-phase mixtures $\alpha - Ta_2C + Ta_6C_5$ and $Ta_6C_5 + TaC_y$ have the lowest free energy, which is why the ordered phases Ta_2C and Ta_3C_2 cannot exist.

Figure 7 shows the calculated equilibrium phase diagram for the Ta–C system in which the ordering of non-stoichiometric cubic TaC_y can occur. The only ordered phase of the non-stoichiometric tantalum carbide TaC_y is the Ta_6C_5 phase with a narrow homogeneity region. A neutron diffraction study [11, 30] showed that in the non-stoichiometric carbide TaC_y, as a result of prolonged slow annealing from 1600 to 750 K, an incommensurate ordered phase forms close to the known M_6C_5-type superstructures. Magnetic susceptibility studies [10] have provided experimental evidence that an ordered phase close to M_6C_5 type forms in tantalum carbide; for the Ta_6C_5–$TaC_{0.83}$ transition, $T_{trans} = 1110$ K.

The calculated values of T_{trans}, ΔS_{trans} and ΔH_{trans} for the Ta_6C_5–TaC_y order–disorder phase transition in non-stoichiometric tantalum carbide are given in table 3.

We note that the position of the phase boundaries on the calculated phase diagram for the Ta–C system can be refined as a result of taking into account the short-range order, which is maintained in the disordered phase TaC_y in a certain temperature range above the order–disorder transition temperature.

5. Superconductivity

Low-temperature measurements showed that the superconductivity temperature T_c of the disordered tantalum carbide TaC_y decreases rapidly with decreasing carbon content: from 10.1 to 1.5 K for $TaC_{1.00}$ and $TaC_{0.83}$, respectively. These results are in a good agreement with published data [3, 31–33] within experimental error (figure 8). The T_c-values of the ordered carbides $TaC_{0.87}$ and $TaC_{0.83}$ turned out to be slightly higher (by 0.3 K and 0.6 K, respectively) than for disordered carbides of the same composition. The observed effect of ordering is not large; so one can only say that there is an incipient tendency of the superconducting temperature T_c to move towards a higher value as a result of the ordering of TaC_y. This distinguishes tantalum carbide from niobium carbide for which the T_c-value of $NbC_{0.83}$ increased several fold upon ordering [4–8]. The different effects or ordering on

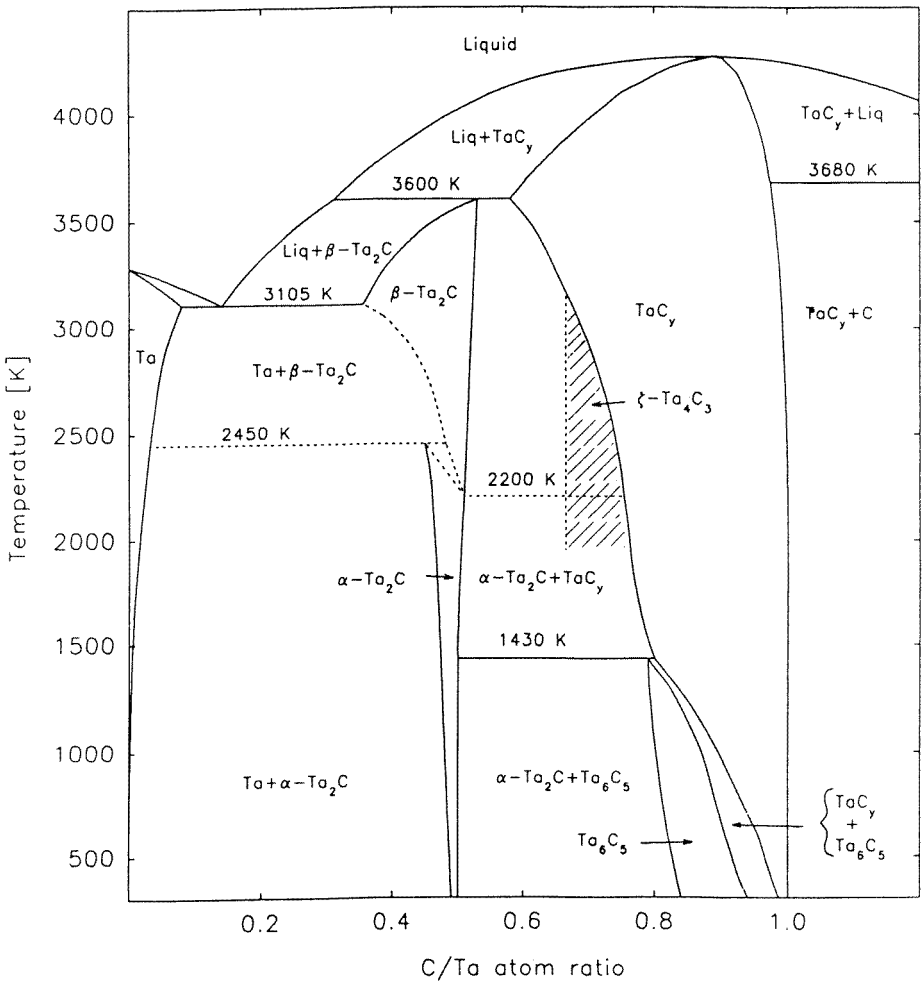

Figure 7. Equilibrium phase diagram of the Ta–C system with consideration of the atomic ordering of non-stoichiometric cubic tantalum carbide TaC_y.

the T_c of these two carbides are presumably due to the differences between the natures of the superstructures that form in them.

In order to explain the superconducting properties of ordered and disordered non-stoichiometric carbides with a base B1-type structure, the quasi-two-dimensional model of superconductivity has been proposed [5, 7]. The main ideas of the model are as follows.

Consider the crystal structure of MC_y. For these compounds in the $[1\bar{1}1]_{B1}$) there is an alternation of metallic and non-metallic atomic planes $(1\bar{1}1)_{B1}$; as noted in sections 3.1 and 3.2, depending on the composition of MC_y, the non-metallic planes may be complete or defective. According to the model in [5–7], superconductivity in non-stoichiometric compounds is due to the presence of quasi-two-dimensional layers consisting of two neighbouring metallic $(1\bar{1}1)_{B1}$ planes and a complete non-metallic $(1\bar{1}1)_{B1}$ plane located between them. The presence of vacancies in the non-metallic planes causes local distortions

Table 3. Thermodynamic characteristics of Ta_6C_5–TaC_y order–disorder phase transitions.

y	T_{trans} (K)	ΔS_{trans} (J mol^{-1} K^{-1})	ΔH_{trans} (kJ mol^{-1})
0.80	1399	1.10	1.54
0.81	1364	1.17	1.59
0.82	1325	1.22	1.61
0.833	1270	1.26	1.60
0.84	1239	1.28	1.58
0.85	1190	1.28	1.52
0.86	1137	1.26	1.43
0.87	1081	1.21	1.31
0.88	1020	1.15	1.17
0.89	955	1.07	1.02
0.90	887	0.98	0.87
0.91	814	0.88	0.72
0.92	738	0.79	0.58
0.93	658	0.69	0.45
0.94	576	0.58	0.34
0.95	489	0.49	0.24

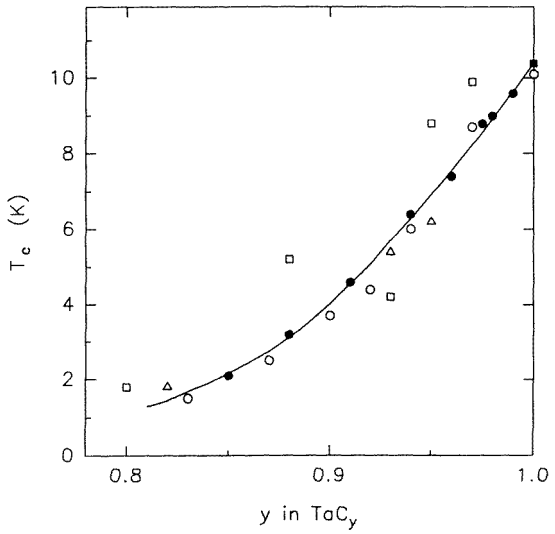

Figure 8. Dependence of the superconducting transition temperature T_c on the composition of a disordered tantalum carbide TaC_y: ○, present paper; ●, from [32]; □, from [3]; ■, from [33]; △, from [31].

of the crystal structure and leads to a deterioration in the superconductive properties of the quasi-two-dimensional layers. In the complete layers the density $N(E_F)$ of electrons states is larger than that in the defective layers. In stoichiometric carbides with a base B1-type structure there are only complete quasi-two-dimensional layers and so these compounds have the highest T_c-values. An increase in the vacancy concentration of a disordered compound leads to an appearance of defective non-metallic $(1\bar{1}1)_{B1}$ planes and defective quasi-two-dimensional layers and is accompanied by a monotonic decrease in $N(E_F)$ and T_c.

In ordered non-stoichiometric carbide with a commensurate M_6C_5-type superstructure, the vacancies are redistributed so that in the non-metallic sublattice complete and defective ordered carbon $(1\bar{1}1)_{B1}$ planes alternate in the $[1\bar{1}1]_{B1}$ direction (figure 5(a)). As a result, a quasi-two-dimensional layered structure arises in the ordered commensurate carbide phase; complete quasi-two-dimensional layers alternate with defective layers and there are periodic local maxima of $N(E_F)$ corresponding to the complete layers. Owing to the presence of complete layers, T_c for an ordered commensurate non-stoichiometric carbide should increase to values close to those for the stoichiometric carbide. Such a change in T_c has indeed been found [4–7] for ordered niobium carbide, in which a commensurate M_6C_6-type superstructure is formed.

As regards TaC_y, this gives rise to an incommensurate superstructure in which, even with the maximum long-range order, the complete quasi-two-dimensional layers are nine to ten times as rare as in the commensurate M_6C_5-type superstructure (figures 5(a) and 5(b)). However, the results of investigation of a base B1-type lattice period (section 3.3) and heat capacity [12, 13] of ordered tantalum carbide show that the maximum degree of order is not reached and that the complete quasi-two-dimensional superconducting layers are almost absent in the ordered tantalum carbide examined. Hence the difference between the superconducting transition temperatures T_c for the ordered incommensurate carbide $TaC_{0.83}$ and the disordered carbide of the same composition is not greater.

If, in the homogeneity region $TaC_{0.79}$–$TaC_{0.89}$ of the ordered phase of tantalum carbide one succeeds in obtaining a commensurate M_6C_5-type superstructure with close to the maximum degree of order, it might be expected that the effect or ordering on T_c will be relatively large and comparable with the T_c change observed on the ordering of niobium carbide.

6. Conclusion

We have presented the results from an experimental study of crystal structure and some properties of non-stoichiometric tantalum carbide in the state with different degrees of long-range order. The neutron diffraction study has shown that an incommensurate superstructure close to M_6C_5 type forms in the non-stoichiometric carbide TaC_y during ordering. This incommensurate superstructure is intermediate between a disordered crystalline structure and some structure which is transformed from the known, completely ordered M_6C_5-type structures with different space groups $C2/m$, $P3_1$ and $C2$. Accurately determining the crystal structure of the ordered tantalum carbide phase calls for diffraction investigations on a high-flux reactor using a high-resolution spectrometer. The results reported show that ordering of carbon atoms and structural vacancies in non-metallic sublattice of tantalum carbide is accompanied by an increase in a base B1-type lattice period and a small increase in the superconducting transition temperature T_c. Calculation of the equilibrium phase diagram of the Ta–C system has shown that tantalum carbide may form only one ordered phase of M_6C_5 type or close to this type.

Acknowledgment

This work was supported by the Russian Foundation for Basic Research under project 95-02-03549a.

References

[1] Gusev A I 1991 *Physical Chemistry of Nonstoichiometric Refractory Compounds* (Moscow: Nauka) (in Russian)
[2] Gusev A I 1991 *Phys. Status Solidi* b **163** 17
[3] Dubrovskaya L B, Rabinkin A G and Geld P V 1972 *Zh. Eksp. Teor. Fiz.* **62** 300
[4] Rempel A A, Gusev A I, Gololobov E M, Prytkova N A and Tomilo Zh M 1986 *Fiz. Tverd. Tela* **28** 279 (Engl. Transl. 1986 *Sov. Phys.–Solid State* **28** 153)
[5] Rempel A A, Gusev A I, Gololobov E M, Prytkova N A and Tomilo Zh M 1987 *Zh. Fiz. Khim.* **61** 1761 (Engl. Trans. 1987 *Russ. J. Phys. Chem.* **61** 919)
[6] Gusev A I and Rempel A A 1988 *Structural Phase Transitions in Nonstoichiometric Interstitial Compounds* (Moscow: Nauka) (in Russian)
[7] Gusev A I and Rempel A A 1989 *Phys. Status Solidi* b **151** 211
[8] Karimov Yu S and Utkina T G 1990 *Pis. Zh. Eksp. Teor. Fiz.* **51** 468 (Engl. Transl. 1990 *JETP Lett.* **51** 528)
[9] Venables J D and Meyerhoff M H 1972 *Solid State Chemistry, Proc. 5th Materials Reserach Symp. (NBS Spec. Publ. 364)* (Washington, DC: US Department of Commerce)
[10] Gusev A I, Rempel A A and Lipatnikov V N 1988 *Phys. Status Solidi* a **106** 459
[11] Rempel A A, Lipatnikov V N and Gusev A I 1990 *Dokl. Akad. Nauk SSSR* **310** 878 (Engl. Transl. 1990 *Sov. Phys.–Dokl.* **35** 103)
[12] Lipatnikov V N, Rempel A A and Gusev A I 1989 *Fiz. Tverd. Tela* **31** 285(Engl. Transl. 1989 *Sov. Phys.–Solid State* **31** 1818)
[13] Gusev A I, Rempel A A and Lipatnikov V N 1996 *Phys. Status Solidi* b **194** 467
[14] Gusev A I 1989 *Phil. Mag.* B **60** 307
[15] Gusev A I 1990 *Fiz. Tverd. Tela* **32** 2752 (Engl. Transl. 1990 *Sov. Phys.–Solid State* **32** 1595)
[16] Gusev A I and Rempel A A 1987 *J. Phys. C: Solid State Phys.* **20** 5011
[17] Gusev A I and Rempel A A 1986 *Phys. Status Solidi* a **93** 71
[18] Kovalev O V 1965 *Irreducible Representations of the Space Groups* (New York: Gordon and Breach)
[19] Gusev A I and Rempel A A 1993 *Phys. Status Solidi* a **135** 15
[20] Lipatnikov V N, Rempel A A and Gusev A I 1996 *Int. J. Refract. Met. Hard Mater.* at press
[21] Rempel A A and Gusev A I 1985 *Kristallografiya* **30** 1112 (Engl. Transl. 1985 *Sov. Phys.–Crystallogr.* **30** 648)
[22] Storms E K and McNeal R J 1962 *J. Phys. Chem.* **66** 1401
[23] Athanassiadis T, Lorenzelli N and de Novion C H 1987 *Ann. Chim.* **12** 129
[24] De Novion C H and Maurce V 1977 *J. Physique Coll.* **38** C7–211
[25] Moisy-Maruce V, de Novion C H, Christensen A N and Just W 1981 *Solid State Commun.* **39** 661
[26] Metzger T H, Peisl J and Kaufmann R 1983 *J. Phys. F: Met. Phys.* **13** 1103
[27] Gusev A I and Rempel A A 1985 *Phys. Status Solidi* b **131** 43
[28] Gusev A I and Rempel A A 1987 *Phys. Status Solidi* b **140** 335
[29] Gusev A I and Rempel A A 1994 *J. Phys. Chem. Solids* **55** 299
[30] Gusev A I Rempel A A and Lipatnikov V N 1991 *Fiz. Tverd. Tela* **33** 2298 (Engl. Transl. 1991 *Sov. Phys.–Solid State* **33** 1295)
[31] Toth L E Ishikawa M and Chang Y A 1968 *Acta Metall.* **16** 1183
[32] Girogi A L Szklarz E G, Storms E K, Bowman A L and Matthias B T 1962 *Phys. Rev.* **125** 837
[33] Pessal N Gold R E and Johansen H A 1968 *J. Phys. Chem. Solids* **29** 19